

doi: 10.12029/gc20220216

贾旭,任俊光,徐文坦,马虎超,张超,石国明. 2022. 大兴安岭多宝山地区晚古生代碱长花岗岩锆石 U-Pb 年龄:对兴安和松嫩地块碰撞拼合时间的限定[J]. 中国地质, 49(2): 586-600.

Jia Xu, Ren Junguang, Xu Wentan, Ma Huchao, Zhang Chao, Shi Guoming. 2022. Zircon U-Pb dating of Late Paleozoic alkali-feldspar granite in Duobaoshan, Daxing'anling Mountains: Constrains on collision and assembly time of Xing'an and Songnen Blocks[J]. Geology in China, 49(2): 586-600(in Chinese with English abstract).

大兴安岭多宝山地区晚古生代碱长花岗岩锆石 U-Pb 年龄:对兴安和松嫩地块碰撞拼合时间的限定

贾旭¹,任俊光¹,徐文坦²,马虎超³,张超⁴,石国明⁵

(1.成都理工大学地球科学学院,四川 成都 610059;2.防灾科技学院地球科学学院,河北 三河 065201;3.金川集团股份有限公司龙首矿,甘肃 金昌 737100;4.西南石油大学地球科学与技术学院,四川 成都 610500;5.黑龙江省地质调查研究总院,黑龙江 哈尔滨 150036)

摘要:【研究目的】大兴安岭多宝山地区位于兴蒙造山带东部的兴安地块与松嫩地块之间的构造带上,区内构造演化复杂,岩浆活动频繁,本文通过对多宝山地区晚古生代碱长花岗岩的年代学和岩石地球化学研究,旨在约束兴安地块与松嫩地块碰撞拼合的时限。【研究方法】开展了 LA-ICP-MS 锆石 U-Pb 测年和岩石主微量元素的测试分析工作。【研究结果】测年获得的 2 件样品的加权平均年龄分别为 (300.3 ± 2.0) Ma 和 (307.3 ± 1.7) Ma,属晚石炭世。岩石具有高硅 $\text{SiO}_2=69.70\% \sim 77.42\%$, 相对富铝 $\text{Al}_2\text{O}_3=11.60\% \sim 15.05\%$, 富钾和钠 ($\text{K}_2\text{O}=4.09\% \sim 5.67\%$; $\text{Na}_2\text{O}=3.13\% \sim 4.13\%$), 贫钙和镁 ($\text{CaO}=0.02\% \sim 0.8\%$; $\text{MgO}=0.02\% \sim 0.48\%$) 的特征;微量元素表现出富集 Rb、Th、Zr 和 Hf, 亏损 Ba、Sr、Nb 和 Ta, ($\text{Zr}+\text{Nb}+\text{Ce}+\text{Y}$) 含量较高,平均值为 529.10×10^{-6} ;稀土元素配分模式呈右倾,具明显 Eu 负异常;同时岩石具有较高的锆石饱和温度,符合 A 型花岗岩的特征。【结论】结合区域构造演化史,认为该期碱长花岗岩为造山期后伸展构造环境下岩浆活动的产物,并指示兴安地块和松嫩地块碰撞拼合的结束。

关键词:晚古生代;碱长花岗岩;年代学;地球化学;构造环境;地质调查工程;多宝山地区;大兴安岭

创新点:厘定多宝山地区晚古生代碱长花岗岩类型;约束兴安地块与松嫩地块碰撞-拼合的时限。

中图分类号:P595;P588.12 文献标志码:A 文章编号:1000-3657(2022)02-0586-14

Zircon U-Pb dating of Late Paleozoic alkali-feldspar granite in Duobaoshan, Daxing'anling Mountains: Constrains on collision and assembly time of Xing'an and Songnen Blocks

JIA Xu¹, REN Junguang¹, XU Wentan², MA Huchao³, ZHANG Chao⁴, SHI Guoming⁵

(1.School of Earth Sciences, Chengdu University of Technology, Chengdu 610059, Sichuan, China; 2.School of Earth Sciences, Institute of Disaster Prevention, Sanhe 065201, Hebei, China; 3. Longshou Mine, Jinchuan Group CO.,LTD.,Jinchang 737100, Gansu, China; 4.School of Geoscience and Technology, Southwest Petroleum University, Chengdu 610500, Sichuan, China; 5. Heilongjiang Geological Survey and Research Institute, Haerbin 150036, Heilongjiang, China)

收稿日期:2019-11-09;改回日期:2022-03-21

基金项目:中国地质调查局项目(DD20160047-07)资助。

作者简介:贾旭,男,1994年生,硕士,主要从事地球化学研究;E-mail: jx3997@outlook.com。

Abstract: This paper is the result of geological survey engineering.

[Objective] The Duobaoshan area of the Greater Xing'an Mountains is located on the tectonic belt between the Xing'an block and the Songnen block in the east of the Xingmeng orogenic belt. In this paper, the chronology and petrogeochemistry of the Late Paleozoic alkali feldspar granites in the Duobaoshan area are used to constrain the time limit of the collision between the Xing'an block and the Songnen block. **[Methods]** In this paper, the zircon U-Pb geochronology and the whole rock geochemistry were carried out. **[Results]** The LA-ICPMS U-Pb ages of zircons from two alkali-feldspar granite samples were (300.3 ± 2.0) Ma and (307.3 ± 1.7) Ma, respectively. Two samples have the similar geochemistry characteristics, with high silicon ($\text{SiO}_2 = 69.70\%$ to 77.42%), relatively high aluminum ($\text{Al}_2\text{O}_3 = 11.60\%$ to 15.05%), and high alkali ($\text{K}_2\text{O} + \text{Na}_2\text{O} = 7.22\%$ to 9.80%), low Ca and Mg ($\text{CaO} = 0.02\%$ to 0.8% , $\text{MgO} = 0.02\%$ to 0.48%), enrichment of Rb, Th, Zr and Hf, depleted of Ba, Sr, Nb and Ta, relatively high (Zr + Nb + Ce + Y). In addition, they also have significantly negative Eu anomalies, with the right-leaning distribution of rare earth elements and high zircon saturation temperature, suggesting both of them are A-type granites. **[Conclusions]** Combined with the regionally tectonical evolution, it is concluded that the alkali-feldspar granite formed at extensional geological background of post-collision regime, marking the end of the collision between the Xing'an block and the Songnen block.

Key words: Late Paleozoic; alkali-feldspar granite; geochronology; geochemical characteristics; tectonic environment; geological exploration engineering; Duobaoshan area; Daxinganling Mountains

Highlights: Determine the type of late Paleozoic alkali-feldspar granite in Duobaoshan area; Constrains the collision and assembly time of Xing'an and Songnen blocks.

About the first author: JIA Xu, male, born in 1994, master, major in geochemical research; E-mail: jx3997@outlook.com.

Fund support: Supported by the project of China Geological Survey (No. DD20160047-07).

1 引言

兴蒙造山带是中亚造山带的重要组成部分,其东段的大兴安岭地区主要包括额尔古纳、兴安与松嫩地块,中生代以来各微地块之间的碰撞拼贴过程一直是地质学研究的热点问题(李双林等,1998;孙德有等,2000;Chen et al.,2000;苗来成等,2003;周长勇等,2005;葛文春等,2005;张兴洲等,2008;隋振民等,2009;刘永江等,2010;赵芝等,2010;赵焕利等,2011;崔芳华等,2013;张磊等,2013;汪岩等,2013;尹志刚等,2018;钱程等,2018;徐文喜等,2018;陈会军等,2019;Ma et al.,2021;赵亮亮等,2021)。近年来,大量学者对兴安与松嫩地块拼接带附近的岩浆岩做了详尽的岩石地球化学、年代学方面的研究工作,但对碰撞拼合的时限及花岗岩岩石类型仍存有争议。其中关于拼合时限有早中生代(Chen et al.,2000;Wu et al.,2002;苗来成等,2003;张彦龙等,2010)和晚古生代(周长勇等,2005;张兴洲等,2008;隋振民等,2009;赵焕利等,2011;崔芳华等,2013;张磊等,2013;杨红章等,2019)之争;多宝山早古生代碱长花岗岩岩石类型亦有S型和A型等不同见解(曲晖等,2011;赵焕利等,2011;郭奎城等,2011)。

本文对黑龙江省多宝山区晚古生代的碱长花岗岩样品进行岩石学、岩石地球化学及锆石 U-Pb 年代学研究,进一步厘定岩石类型、成因及形成构造背景,以期对兴蒙造山带东段的构造演化提供重要信息。

2 地质概况及岩石学特征

多宝山区位于大兴安岭东北部,地处兴蒙造山带东段的兴安地块与松嫩地块拼合带附近(图1)。区内发育的地层由老到新依次为:下—中奥陶统铜山组(O_{1-2t})、下—中奥陶统多宝山组(O_{1-2d})、上奥陶统裸河组(O_3l)、下志留统黄花沟组(S_1h)、顶志留—中泥盆统泥鳅河组(S_4D_2n)、下白垩统的龙江组(K_1l)、光华组(K_1gh)、九峰山组(K_1j)、甘河组(K_1g)以及大面积的第四系河流堆积物和洪积物。区域上地质构造复杂,岩浆活动频繁,从加里东期—燕山早期均有不同规模的岩浆活动,形成了大量酸性侵入岩体,同时岩石类型多变,由老到新分布有中奥陶世的花岗闪长岩、花岗闪长斑岩,早石炭世的正长花岗岩,晚石炭世—早二叠世的碱长花岗岩,中—晚三叠世的花岗闪长岩,早—中侏罗世的花岗闪长岩、二长花岗岩,早白垩世的花岗斑岩及

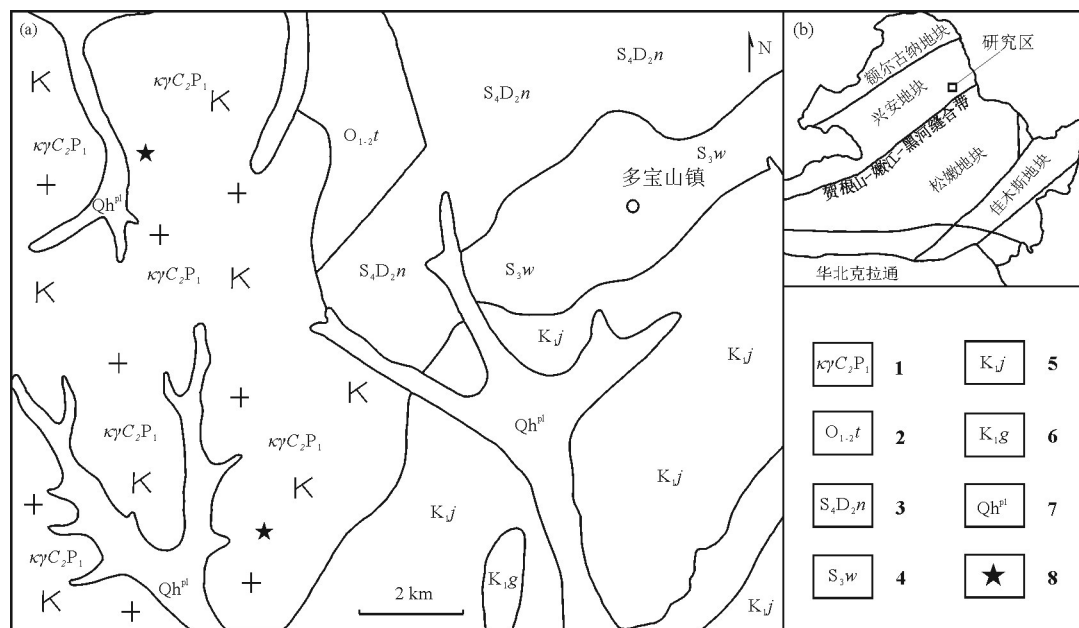


图1 多宝山区地质简图(a)及区域构造简图(b)

1—早二叠世碱长花岗岩;2—下一中奥陶统铜山组;3—顶志留—中泥盆统泥鳅河组;4—上志留统卧都河组;5—下白垩统九峰山组;6—下白垩统甘河组;7—河流堆积物;8—锆石样品位置

Fig. 1 Simplified geological map (a) and tectonic setting map (b) of Dobaoshan area

1—Early Permian alkali feldspar granite;2—Lower—middle Ordovician Tongshan Formation;3—Upper Silurian—Middle Devonian Niquihe Formation;4—Upper Silurian Woduhe Formation;5—Lower Cretaceous Jiufengshan Formation;6—Lower Cretaceous Ganhe Formation;7—River deposits;8—Zircon sampling location

不同期次的岩脉。

本文研究的晚古生代碱长花岗岩主要发育在多宝山地区西南侧,群富村以西一带,岩体大致呈N—NNE向展布,出露面积约60 km²。其岩相学特征揭示:岩石具粗中粒结构,块状构造。岩石主要成分为碱性长石(63%±)、石英(30%±)、斜长石(5%±)、少量黑云母、副矿物(2%±)粒度小于6 mm。其中碱性长石为微斜条纹长石,发育纹状条纹、格子双晶结构,晶粒包裹少量净边结构的斜长石微粒(图2);斜长石为半自形柱状,聚片双晶发育,成分An为27的更长石,被碱性长石交代,裂纹发育,粒度为0.1~1.5 mm,交代斜长石具交代蚕食结构,粒度为0.2~5.5 mm;石英主要为他形粒状,部分细粒化,可见波状消光,变形条带发育,交代长石者为交代蚕食结构,裂纹发育,粒度小于6 mm;黑云母为片状,晶面完全被褐铁矿交代,片径小于0.2 mm。副矿物组合为:锆石、磷灰石、黄铁矿、锐钛矿、磁铁矿、白钛石、榍石、辉石、绿帘石、石榴石、角闪石及褐铁矿。

3 样品及测试方法

本文对2件样品PM104U—Pb(采样位置:125°33'57.82"E;50°1'10.5"N)和PM116U—Pb(采样位置:125°32'30.47"E;50°7'19.83"N)进行LA—ICP—MS锆石U—Pb法年龄的测定,另在研究区碱长花岗岩体的不同部位采集13件样品进行岩石地球化学的分析测试。

野外采集测年样品重约10 kg,锆石分选在河北省区域地质矿产调查研究所完成,用常规方法先将样品粉碎至80~100目,将过筛后的岩石粉末进行淘洗,去除轻矿物部分,保留重砂部分,后经过电磁选得到纯度较高的单矿物样品。在双目镜下挑选出晶形、透明度较好、裂隙和包体较少、表面洁净的锆石颗粒用于年龄测定。锆石制靶和阴极发光(CL)图像的采集在北京离子探针中心完成。锆石U—Pb同位素分析在中国地质调查局天津地质调查中心完成,检测依据为DZ/T0184.3—1997,所用仪器为ThermoFischer公司制造的Neptune型LA—MIC—

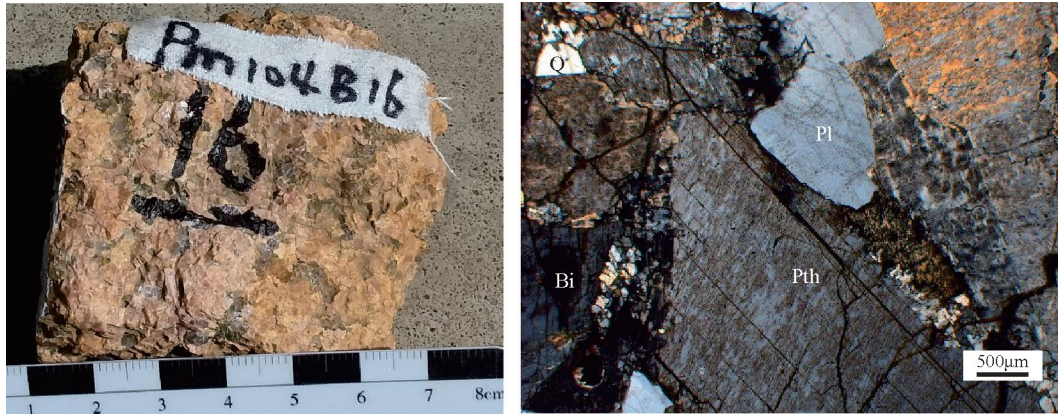


图2 粗中粒碱长岩的岩石手标本和镜下特征
Q—石英;Pl—斜长石;Pth—条纹长石;Bi—黑云母

Fig.2 Rock hand specimens and microphotograph features of coarse and medium-grained alkali feldspars
Q—Quartz;Pl—Plagioclase; Pth—Perthite; Bi—Biotite

ICP-MS 和 Cetac 公司制造的 GeolasPro193 准分子型激光系统,用 193 nm 激光器对锆石进行剥蚀,深度为 20~40 µm,激光剥蚀斑束直径为 35 µm,应用 TEMORA 和 GJ-1 作为外部锆石年龄标准进行分馏校正,详细的实验原理和流程见相关文献(李怀坤等, 2009)。数据处理采用 Glitter(Jackson,2004)程序计算锆石表面年龄及标准偏差;使用 Isoplot 3.0 (Ludwig,1991)程序进行锆石样品的年龄谱和图投图和加权平均年龄值计算。

13 件新鲜、无蚀变样品的主量-微量-稀土元素的分析测试在中国地质调查局天津地质调查中心完成,其中主量元素分析采用 X-荧光光谱法测定(XRF),所用仪器型号为 PW2400/40 型 X-荧光光谱仪(荷兰帕纳科公司)。微量及稀土元素分析采用电感耦合等离子质谱法(ICP-MS)测定,仪器型号为 X Series II 型电感耦合等离子体质谱仪(美国热电公司)。

4 测试结果和分析

锆石 CL 图像(图3)显示锆石具有较好的晶形,整体多为自形、半自形粒状,晶棱和晶面相对清晰,可见自形生长纹和生长环带,长宽比较小,多数为 1:1~2:1。参与加权年龄计算的锆石 Th/U 比值分别介于 0.30~1.34(样品 PM104U-Pb,均值 0.45)和 0.36~0.75(样品 PM116U-Pb,均值 0.43),比值均大于 0.1,据此可以推断锆石性质为岩浆成因(吴元保等, 2004)。

本次对样品 PM104U-Pb 和 PM116U-Pb 均进行了 25 个点的测年分析(表 1),剔除年龄谐和度低于 95%的锆石后,年龄数据投影点落在谐和线上或附近,表明这些颗粒形成后 U-Pb 同位素体系是封闭的,基本没有 U 或 Pb 同位素的丢失或加入。样品 PM104U-Pb 的 20 颗锆石的 ²⁰⁶Pb/²³⁸U 年龄介于(297±4)Ma~(304±4)Ma,计算加权年龄为(300.3±2.0)Ma

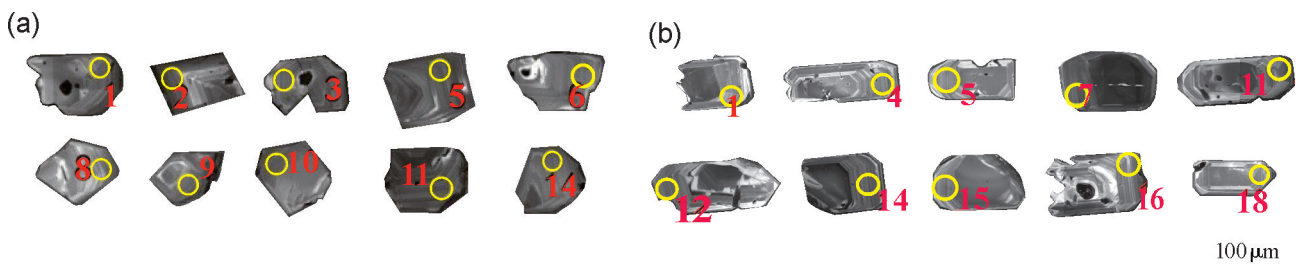


图3 样品 PM104U-Pb(a)与 PM116U-Pb(b)锆石阴极发光图像
Fig.3 CL images of zircons of PM104U-Pb(a) and PM116U-Pb(b)

表1 多宝山碱长花岗岩LA-ICP-MS锆石U-Pb测年分析结果

Table 1 LA-ICP-MS zircon U-Pb dating results for the alkali-feldspar granite in Duobaoshan

测点号	元素含量/ 10^{-6}		Th/U	同位素比值				年龄/Ma				谐和度/%
	Th	U		$^{207}\text{Pb}/^{235}\text{U}$	1σ	$^{206}\text{Pb}/^{238}\text{U}$	1σ	$^{207}\text{Pb}/^{235}\text{U}$	1σ	$^{206}\text{Pb}/^{238}\text{U}$	1σ	
样品PM104 U-Pb												
1	132.29	328.7	0.40	0.3469	0.012	0.0482	0.0009	302.42	8.83	303.47	5.4	99
2	270.85	677.2	0.40	0.3827	0.01	0.0478	0.0008	329.04	7.67	300.83	4.89	96
3	139.51	326	0.43	0.3441	0.01	0.0478	0.0008	300.28	7.54	300.94	4.76	99
4	244.94	570.6	0.43	0.4312	0.017	0.0476	0.0007	364.04	12.2	299.73	4.07	80
5	323.79	835	0.39	0.3433	0.009	0.0481	0.0007	299.67	6.66	302.95	4.38	98
6	145.16	411.1	0.35	0.3372	0.009	0.0472	0.0007	295.01	6.57	297.01	4.27	99
7	185.51	331.3	0.56	0.4955	0.025	0.0487	0.0009	408.68	17	306.25	5.64	71
8	136.89	412.1	0.33	0.3384	0.009	0.0478	0.0008	296	6.85	301.23	4.89	98
9	158.77	435.6	0.36	0.3386	0.011	0.0474	0.0006	296.13	8.33	298.64	3.84	99
10	179.38	514	0.35	0.3423	0.01	0.0474	0.0006	298.94	7.64	298.82	3.83	99
11	225.63	668.8	0.34	0.3414	0.008	0.0482	0.0008	298.2	5.82	303.32	4.87	98
12	340.21	850.8	0.40	0.349	0.01	0.0478	0.0007	303.94	7.53	301.12	4.51	99
13	629.28	471.2	1.34	0.3402	0.008	0.0477	0.0008	297.35	5.98	300.18	4.84	99
14	111.59	357.9	0.31	0.349	0.012	0.0482	0.0007	303.99	8.65	303.55	4.2	99
15	122.72	304.2	0.40	0.3728	0.02	0.0489	0.0006	321.72	14.7	307.76	3.88	91
16	452.79	1218	0.37	0.3735	0.01	0.0472	0.0007	322.28	7.13	297.08	4.27	95
17	146.08	376.4	0.39	0.3531	0.011	0.0479	0.0007	307.08	7.85	301.83	4.1	98
18	96.99	318.8	0.30	0.4254	0.017	0.0489	0.0007	359.93	12.1	307.69	4.46	84
19	141.9	346.1	0.41	0.3466	0.01	0.0476	0.0006	302.13	7.34	299.96	3.87	99
20	155.32	356.9	0.44	0.3364	0.014	0.0474	0.0007	294.46	10.9	298.47	4.56	98
21	192.02	450.9	0.43	0.3419	0.012	0.0473	0.0006	298.6	8.96	297.91	3.74	99
22	337.38	787.7	0.43	0.3502	0.008	0.0475	0.0007	304.88	5.96	299.18	4.47	98
23	345.09	738.1	0.47	0.346	0.009	0.0474	0.0007	301.67	6.55	298.6	4.5	98
24	296.5	402.1	0.74	0.3426	0.01	0.0478	0.0006	299.16	7.76	301.26	3.89	99
25	112.15	165.4	0.68	0.0182	0.047	0.0009	0.415	333.07	13.3	297	5.63	88
样品PM116 U-Pb												
1	121.23	293.9	0.41	0.368	0.01	0.0497	0.0007	318	7.12	312	4.33	98
2	169.36	408.9	0.41	0.3628	0.012	0.0482	0.0006	314	8.96	303	3.93	96
3	147.04	342.3	0.43	0.35	0.01	0.0493	0.0008	305	7.76	310	5.14	98
4	147.57	340.2	0.43	0.3661	0.012	0.0494	0.0007	317	8.93	311	4.52	98
5	139.22	326.2	0.43	0.3505	0.011	0.0485	0.0007	305	8.50	305	4.23	99
6	113.55	310.9	0.37	0.3389	0.011	0.0482	0.0007	296	8.04	303	4.24	97
7	130.21	352.4	0.37	0.365	0.011	0.0487	0.0007	316	8.36	307	4.25	97
8	122.83	311.7	0.39	0.3674	0.015	0.0492	0.0007	318	11.35	309	4.39	97
9	143.99	316	0.46	0.3562	0.014	0.0494	0.0008	309	11.55	311	4.85	99
10	125.83	296.5	0.42	0.3404	0.01	0.0495	0.0007	297	7.88	311	4.20	95
11	96.65	257.2	0.38	0.3543	0.012	0.0493	0.0007	308	9.25	310	4.07	99
12	112.42	276.7	0.41	0.3565	0.011	0.0492	0.0008	310	7.97	310	4.88	99
13	106.89	275.2	0.39	0.3785	0.015	0.0491	0.0008	326	11.35	309	4.78	94
14	124.4	343	0.36	0.3664	0.012	0.0495	0.0007	317	9.00	311	4.52	98
15	222.91	393.9	0.57	0.3613	0.011	0.0491	0.0008	313	8.41	309	4.68	98
16	100.48	243.4	0.41	0.3431	0.014	0.0494	0.0006	300	10.67	311	3.89	96
17	154.83	353.1	0.44	0.3552	0.012	0.0489	0.0007	309	8.58	308	4.60	99
18	154.2	336.1	0.46	0.3729	0.012	0.0491	0.0007	322	8.63	309	4.44	95
19	297.45	393.4	0.76	0.3533	0.012	0.048	0.0006	307	8.64	303	3.88	98
20	100.8	271.1	0.37	0.332	0.011	0.0483	0.0006	291	8.54	304	3.75	95
21	122.89	292.7	0.42	0.3432	0.011	0.0482	0.0006	300	8.14	303	3.87	98
22	155.63	356	0.44	0.3633	0.013	0.0486	0.0007	315	9.30	306	4.35	97
23	2491.7	1035	0.37	0.4439	0.01	0.0477	0.0011	373	6.96	300	6.54	78
24	123.11	288.2	0.43	0.3547	0.013	0.0478	0.0007	308	9.57	301	4.35	97
25	136.11	342.3	0.40	0.3366	0.012	0.0478	0.0008	295	8.71	301	4.68	97

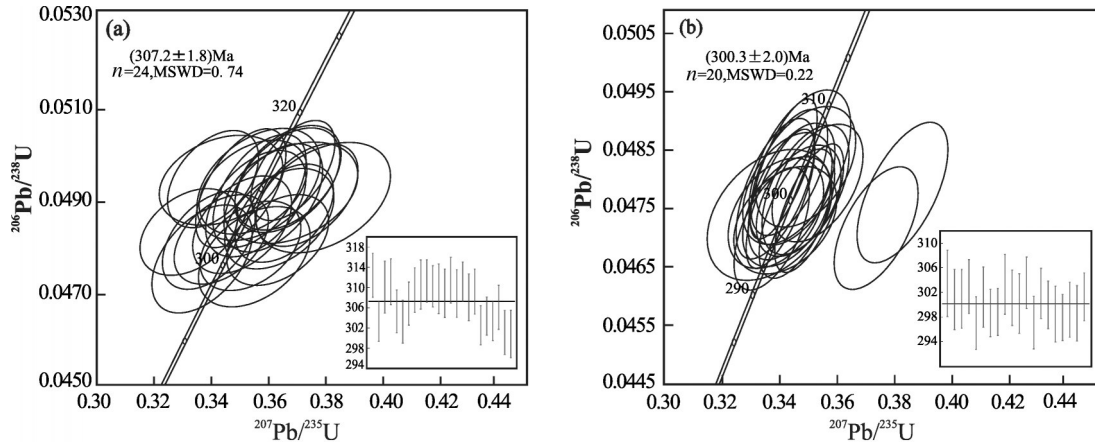


图4 样品PM104U-Pb(a)与PM116U-Pb(b)锆石U-Pb年龄谐和图
Fig.4 Zircon U-Pb age concordia diagrams of PM104U-Pb(a) and PM116U-Pb(b)

($\text{MSWD}=0.22$) (图4a)。样品PM116U-Pb的24颗锆石的 $^{206}\text{Pb}/^{238}\text{U}$ 年龄介于 $(330 \pm 4) \text{ Ma}$ ~ $(312 \pm 4) \text{ Ma}$, 计算加权年龄为 $(307.3 \pm 1.7) \text{ Ma}$ ($\text{MSWD}=0.71$) (图4b)。

5 岩石地球化学特征

5.1 主量元素特征

从表2中数据可知,该碱长花岗岩样品主量元素中 SiO_2 含量为69.70%~77.42%, TiO_2 含量为0.08%~0.34%, Al_2O_3 含量为11.60%~15.05%, Fe_2O_3 含量为0.27%~2.46%, FeO 含量为0.51%~0.93%, MnO 含量为0.01%~0.09%, MgO 含量为0.02%~0.48%, CaO 含量为0.02%~0.8%, Na_2O 含量为3.13%~4.13%, K_2O 含量为4.09%~5.67%, P_2O_5 含量0.01%~0.06%,整体上具有高硅、富钾和钠及贫钙、镁、磷特点。

全碱含量高, ($\text{Na}_2\text{O}+\text{K}_2\text{O}$) 介于7.22%~9.8%, 平均值8.43%; $\text{K}_2\text{O}/\text{Na}_2\text{O}$ 介于1.07~1.51, 在 $\text{K}_2\text{O}-\text{SiO}_2$ 图解(图5a)中表现为高钾钙碱性。碱度率 AR 介于2.43~4.97, 为碱性系列岩石。 A/NK 介于1.07~1.53, $A/\text{CNK}=1.05\sim 1.45$, 在铝饱和指数判别图解(图5b)中投点均落入过铝质区内。 FeO^T 介于0.99~2.77, $\text{FeO}^\text{T}/\text{MgO}$ 值变化较大介于5.78~83.04, 表现出富Fe特点。镁指数 $\text{Mg}^\text{#}$ 介于1.19~14.71, 表明其可能是由地壳物质部分熔融组成(Rapp et al., 1995)。

5.2 微量与稀土元素特征

样品的微量与稀土元素含量见表2, 大离子亲石元素(LILE)中Rb、Sr、Ba含量分别为 58×10^{-6} ~ 200×10^{-6} 、 10×10^{-6} ~ 99×10^{-6} 、 9×10^{-6} ~ 436×10^{-6} ; 高场强元素(HFSE)Nb、Ta、Zr、Hf含量分别为 $10.4 \times$

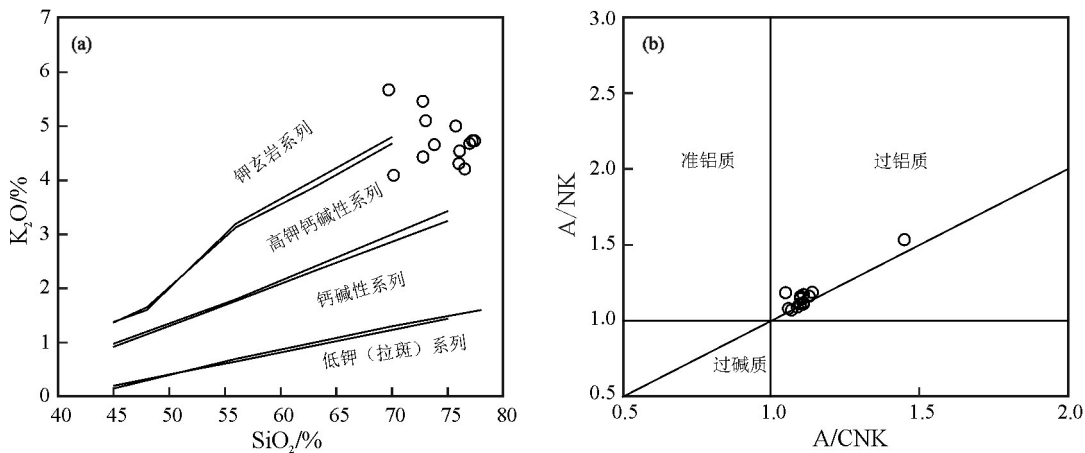


图5 多宝山碱长花岗岩 $\text{K}_2\text{O}-\text{SiO}_2$ (a, 据 Peccerillo et al., 1976)与 $A/\text{NK}-A/\text{CNK}$ 图解(b, 据 Maniar et al., 1989)
Fig.5 $\text{K}_2\text{O}-\text{SiO}_2$ (a, after Peccerillo et al., 1976) and $A/\text{NK}-A/\text{CNK}$ (b, after Maniar et al., 1989) diagrams of the alkali-feldspar granite in Duobaoshan

表2 多宝山碱长花岗岩主量、微量和稀土元素岩石化学分析结果及相关参数

Table 2 Major, rare earth and trace element of alkali-feldspar granite in Duobaoshan

样品号	Pm119	Pm119	Pm119	Gs	Pm118	Pm118	Pm118	Pm118	Pm116	Pm104	Pm104	Pm104	Gs
	Gs48	Gs46	Gs23	6606	Gs33	Gs29	Gs137	Gs131	Gs40	Gs33	GS28	Gs15	2161A
SiO ₂	76	76.52	76.06	72.78	70.14	73.8	69.7	73.02	72.76	77.42	76.96	77.22	75.72
TiO ₂	0.12	0.13	0.18	0.31	0.34	0.19	0.34	0.23	0.21	0.08	0.08	0.09	0.17
Al ₂ O ₃	12.13	11.92	12.8	13.46	14.7	13.49	15.05	13.21	13.93	11.6	11.81	11.7	13.26
Fe ₂ O ₃	1.63	1.55	1.09	1.9	2.46	1.47	1.99	1.73	1.5	1.02	1.38	0.99	0.27
FeO	0.62	0.51	0.51	0.75	0.56	0.59	0.57	0.81	0.93	0.78	0.63	0.77	0.75
MnO	0.09	0.05	0.02	0.06	0.07	0.05	0.02	0.06	0.04	0.03	0.02	0.02	0.01
MgO	0.03	0.13	0.05	0.3	0.48	0.12	0.11	0.11	0.13	0.04	0.03	0.02	0.08
CaO	0.02	0.1	0.07	0.8	0.31	0.35	0.23	0.24	0.39	0.03	0.04	0.03	0.25
Na ₂ O	4.04	3.93	4.01	3.98	3.13	4	4.13	3.4	3.62	3.23	3.33	3.4	3.74
K ₂ O	4.31	4.21	4.54	4.43	4.09	4.66	5.67	5.1	5.46	4.73	4.68	4.73	5
P ₂ O ₅	0.02	0.02	0.03	0.08	0.04	0.04	0.06	0.03	0.03	0.02	0.02	0.01	0.03
烧矢量	0.4	0.32	0.46	0.52	3.14	0.66	1.62	1.64	0.62	0.48	0.6	0.38	0.38
总量	99.41	99.39	99.82	99.37	99.46	99.42	99.49	99.58	99.61	99.45	99.58	99.35	99.67
Na ₂ O+K ₂ O	8.35	8.14	8.55	8.41	7.22	8.66	9.8	8.5	9.08	7.96	8.01	8.13	8.74
K ₂ O/Na ₂ O	1.07	1.07	1.13	1.11	1.31	1.17	1.37	1.5	1.51	1.46	1.41	1.39	1.34
FeO ^f	2.09	1.9	1.49	2.46	2.77	1.91	2.36	2.37	2.28	1.7	1.87	1.66	0.99
FeO ^f /MgO	83.47	14.65	29.23	8.2	5.78	15.94	21.46	21.52	17.54	47.16	58.49	83.04	12.26
A/NK	1.07	1.08	1.11	1.19	1.53	1.16	1.16	1.19	1.17	1.11	1.12	1.09	1.15
A/CNK	1.07	1.06	1.1	1.05	1.45	1.1	1.13	1.14	1.11	1.11	1.11	1.09	1.1
Mg ^f	0.02	0.11	0.06	0.18	0.24	0.1	0.08	0.08	0.09	0.04	0.03	0.02	0.13
Rb	143	143	135	110	130	141	76	82	58	200	194	188	104
Sr	16	18	32	99	80	77	21	36	29	10	12	17	33
Ba	81	67	201	289	436	368	132	171	108	9	28	31	81
Nb	32.4	32.1	28.7	24.9	21.3	26.3	23.5	18	10.4	44.5	29.6	34.6	20.4
Ta	2.87	3.09	1.68	2.34	1.34	2.73	1.31	1.04	0.52	4.69	3.82	3.32	1.79
Zr	390	370	345	316	207	201	642	401	380	321	278	295	333
Hf	8	9.1	8.1	6.6	4.8	5.1	11.9	7.7	6.8	8.9	7.3	7.4	7.6
Th	16.8	15.5	13.1	11.9	13.9	15.2	14.9	9.28	8.62	19.3	12.5	16.7	13.7
Cr	31.2	8.1	38.2	13	37.9	39	2.6	21.7	23.6	31.3	8.8	26.9	11.4
Sc	5.65	5.22	5.17	4.88	6.25	4.65	6.85	4.06	5.56	1.88	1.9	1.83	4.13
U	2.38	2.28	0.85	2.27	2.19	2.13	1.31	0.86	0.8	3.95	3.66	3.33	2.83
Rb/Sr	8.94	7.94	4.22	1.11	1.63	1.83	3.62	2.28	2	20	16.17	11.06	3.15
Rb/Ba	1.77	2.13	0.67	0.38	0.3	0.38	0.58	0.48	0.54	22.22	6.93	6.06	1.28
Zr/Hf	48.75	40.66	42.59	47.88	43.13	39.41	53.95	52.08	55.88	36.07	38.08	39.86	43.82
La	28	24.4	42.1	48.5	24.7	11	143	58.5	56.4	6.17	5.47	15.3	69.9
Ce	103	86.2	97.4	108	80.5	67.4	309	165	139	45.5	47.3	93.1	153
Pr	8.52	7.17	10.9	13	6.02	3.08	33.5	14.1	14.8	1.7	1.37	3.82	17.1
Nd	32.5	27.3	42.9	49.9	22.4	11.4	120	51	54.6	6	4.88	13.4	62.2
Sm	7.51	6.13	7.22	10.3	4.3	2.47	16.6	8.18	8.34	1.31	1.19	2.84	10.2
Eu	0.46	0.38	0.71	0.84	0.75	0.58	0.42	0.46	0.35	0.03	0.03	0.07	0.26
Gd	8.68	7.22	6.07	9.88	4.41	3	11.5	6.59	5.87	1.84	1.79	3.54	8.72
Tb	1.68	1.44	0.89	1.6	0.8	0.65	1.39	0.92	0.75	0.61	0.54	0.94	1.24
Dy	11.1	9.71	5.04	9.45	5.11	4.83	6.73	5.1	3.71	6.38	5.15	8.14	6.81
Ho	2.37	2.07	1	1.91	1.07	1.14	1.19	1	0.67	1.89	1.44	2.08	1.32
Er	7.32	6.39	3.01	5.62	3.23	3.89	3.09	2.92	1.84	7.66	5.5	7.28	3.82
Tm	1.07	0.93	0.45	0.79	0.47	0.66	0.41	0.42	0.26	1.29	0.94	1.14	0.54
Yb	6.82	6.07	3.09	4.78	2.87	4.62	2.68	2.71	1.75	8.66	6.37	7.43	3.49
Lu	1.13	0.96	0.53	0.71	0.43	0.75	0.47	0.47	0.3	1.41	1.03	1.19	0.59
Y	71.5	62.9	29.3	54.6	30.3	35.5	29.6	26.6	17.3	54.9	43	62.5	40.1
ΣREE	220.16	186.37	221.31	265.28	157.06	115.47	649.98	317.37	288.64	90.45	83	160.27	339.19
LREE/HREE	4.48	4.36	10.02	6.64	7.54	4.91	22.67	14.77	18.05	2.04	2.65	4.05	11.79
δEu	0.17	0.17	0.32	0.25	0.52	0.65	0.09	0.19	0.15	0.06	0.06	0.06	0.08
δCe	1.59	1.55	1.07	1.02	1.54	2.75	1.04	1.34	1.13	3.33	4.05	2.86	1.04
(La/Yb) _n	2.77	2.71	9.19	6.84	5.8	1.61	35.97	14.55	21.73	0.48	0.58	1.39	13.5
Zr+Nb+Ce+Y	596.9	551.2	500.4	503.5	339.1	330.2	1004.1	610.6	546.7	465.9	397.9	485.2	546.5
锆石饱和温度	794.73	824.72	869.45	912.51	833.2	826.6	841.8	845.67	861.41	902.78	832.25	858.43	844.7

注:主量元素质量分数单位为%,微量元素含量单位为g/t,锆石饱和温度单位为°C。

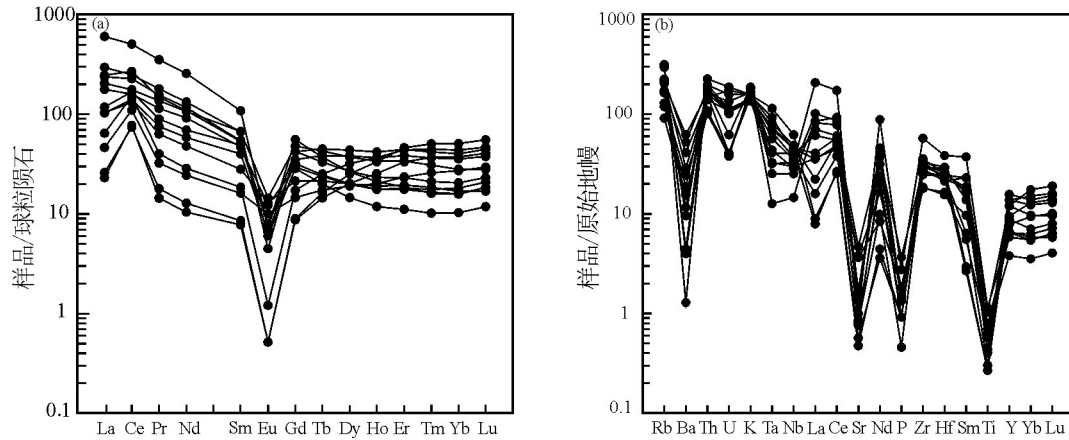


图6 多宝山碱长花岗岩稀土元素球粒陨石标准化配分曲线图(a)及微量元素原始地幔标准化蛛网图(b)
(标准化数值据Sun et al.,1989)

Fig.6 Chondrite-normalized REE patterns (a)and primitive mantle-normalized trace element patterns(b) of the alkali-feldspar granite in Duobaoshan(normalized data after Sun et al.,1989)

10^{-6} ~ 44.5×10^{-6} 、 0.52×10^{-6} ~ 4.69×10^{-6} 、 201×10^{-6} ~ 642×10^{-6} 、 4.8×10^{-6} ~ 11.9×10^{-6} ;放射性生热元素(RPH)U、Th含量分别为 0.8×10^{-6} ~ 3.95×10^{-6} 、 8.62×10^{-6} ~ 19.3×10^{-6} 。

微量元素对原始地幔标准化蛛网图(图6b)上,表现出Rb、Th、K、Nd、Zr、Hf元素的富集和Ba、Sr、P、Ti的亏损,表明岩浆在演化过程中存在金红石、磷灰石以及钛铁矿的残留或分离结晶(康磊等,2016)。Nb/Ta值为8~20,均值为13.02,接近大陆地壳的Nb/Ta比值10~14(赵振华等,2008),但低于上地幔Nb/Ta的平均值17.5(McDonough et al.,1995)。Rb/Sr比值为1.11~20,平均为6.46,明显高于原始地幔的Rb/Sr值0.03,且大于地壳的Rb/Sr平均值0.24(黎彤,1994),上述比值均表明花岗岩可能为壳源。

稀土总量(REE)为 126×10^{-6} ~ 679.58×10^{-6} ,平均值为 280.97×10^{-6} ,其中轻稀土元素(LREE)含量为 60.71×10^{-6} ~ 622.52×10^{-6} ,平均值为 211.80×10^{-6} ;重稀土元素(HREE)含量为 15.15×10^{-6} ~ 40.17×10^{-6} ,平均值为 26.25×10^{-6} ;轻稀土与重稀土元素含量的比值(LREE/HREE)为2.04~22.67,平均值8.77,为轻稀土富集型。 La_N/Yb_N 值为0.48~35.98,均值为9.58,表明轻、重稀土元素分馏较明显。 δEu 为0.05~0.65,均值为0.21,表现出明显的Eu负异常,可能是在岩体演化过程中斜长石结晶分异作用强烈造成的。 δCe 介于1.02~4.05,均值为1.87,存在弱正Ce异常。球粒

陨石标准化的稀土元素配分模式表现为轻稀土元素富集的右倾“海鸥型”(图6a)。

6 讨论

6.1 形成时代

前人对多宝山区碱长花岗岩的研究工作相对较少,在卧都河幅(1:25万)地质调查工作中将其归属为华力西晚期白岗质花岗岩,但其数据分散,不够精确,可信度较差。赵焕利等(2011)及曲晖等(2011)对区内3件碱长花岗岩样品进行了单颗粒锆石U-Pb法定年,获得年龄值分别为 (300 ± 3) Ma、 (304 ± 2) Ma和 (309 ± 3) Ma。本次定年结果显示2件碱长花岗岩样品的加权年龄为 (300.3 ± 2.0) Ma(MSWD=0.22, $n=20$)和 (307.3 ± 1.8) Ma(MSWD=0.74, $n=24$),与前人所得年龄数据基本一致,可将其形成时代限定为300~310Ma,为晚华力西期晚石炭世岩浆活动的产物。

6.2 岩石成因类型

Loiselle and Wones(1979)将非造山环境下形成的花岗岩称为A型花岗岩,以碱性(Alkaline)、贫水(Anhydrous)和非造山(Anorogenic)的首字母命名。但长久以来,对A型花岗岩的判定目前存在着不少争议,综合来说可通过矿物学和岩石地球化学特征来对A型花岗岩进行判定。矿物学特征上,A型花岗岩主要的矿物组合为碱性长石(钾长石)、石英及(富Fe)镁铁质暗色矿物,斜长石缺失或含量很

少(顾连兴,1990),常在岩浆作用晚期形成霓石、霓辉石、钠闪石、钠铁闪石、萤石、富氟的稀土矿物及富钍锆石等特征矿物(吴锁平等,2007;李小伟等,2010)。地球化学特征上,A型花岗岩在主量元素上主要表现为富Si,富K($K_2O > 4\%$),贫Ca、Mg(张旗等,2012)。元素组合上($K_2O + Na_2O$)/CaO、 K_2O/Na_2O 、 FeO^T/MgO 值均较高(Whalen et al.,1987)。微量元素上主要表现为富集高场强元素Nb、Ta、Zr、Hf、Th,亏损Ba、Sr、P、Ti,且 $(Zr + Nb + Ce + Y) > 350 \times 10^{-6}$ (Whalen et al.,1987)。稀土元素总量高,常为轻稀土元素富集型(陈培荣等,1998),配分模式常呈“右倾海鸥型”展布并伴随有明显的Eu负异常(贾小辉等,2009)。

本区碱长花岗岩以碱性长石、石英为主要造岩矿物,斜长石含量很少,副矿物包含有锆石、磷灰石和磁铁矿等,镜下未见白云母、堇青石等S型花岗岩类富铝特征矿物。

岩石地球化学方面,样品主量元素以高Si(均值74.47%)、富K(均值4.73%)、贫Ca和Mg(均值0.22%和0.13%)、相对富Al(均值13.00%)为主要特征; $(K_2O + Na_2O)/CaO$ 介于10.51~417.50,比值较高且变化范围较大; K_2O/Na_2O 介于1.07~1.51,表现出富钾特征; FeO^T/MgO 介于5.78~83.04,远高于一般I型(均值2.27)、S型(均值2.38)及M型(均值2.37)花岗岩类(Whalen et al.,1987)。微量元素蛛网图显示该岩体样品富集大离子亲石元素Rb、U、K和高场强元素Zr、Hf等,亏损Ba、Nb、Ta、Sr、P、Ti元素; $(Zr + Nb + Ce + Y)$ 介于 $330.2 \times 10^{-6} \sim 1004.1 \times 10^{-6}$,均值 529.1×10^{-6} ,远大于S型、I型花岗岩的平均值(分别为 235×10^{-6} 和 247×10^{-6})(刘昌实等,2003)。 δEu 均值为0.21, Eu负异常明显,稀土元素配分模式表现为轻稀土元素富集的右倾型。

实验岩石学资料和锆石饱和温度已证明(Clemens et al.,1986; King et al.,1997)A型花岗岩通常形成于高温低压环境(Breiter.,2011)。本文利用锆石地质温度计公式(Watson,1979)计算锆石饱和温度为794.73~912.51℃,平均值849.87,符合A型花岗岩形成温度比I型花岗岩(764℃)一般较高的特点,也相适于中国东北地区晚古生代A型花岗岩锆石饱和温度的范围(843~921℃)(隋振民等,2011)。

综合上述矿物学、岩石地球化学及结晶温度特

征认为该期碱长花岗岩为A型花岗岩。同样在 Na_2O-K_2O 图解、 $(K_2O + Na_2O)/CaO-(Zr + Nb + Ce + Y)$ 图解和 $FeO^T/MgO-(Zr + Nb + Ce + Y)$ 判别图解中(图7a~c),大多数样品均投影于A型花岗岩区域。

6.3 构造意义

传统意义上A花岗岩的构造背景被定义为“非造山”的张性环境。Eby(1992)在系统总结A型花岗岩的岩石学和地球化学特征之后,将其进一步分为 A_1 和 A_2 型两个亚类,前者源自地幔,代表大陆裂谷环境和地幔热柱/热点环境;后者系由地壳或岛弧派生,代表碰撞后或造山后的张性构造环境。对应的洪大卫等(1995)根据野外地质特征、岩石学特征及地球化学特征将A型花岗岩分为非造山和后造山花岗岩。因Y/Nb比值对于A型花岗岩而言比较稳定,因此可据此判别其成因类型(Eby,1992),当其值小于1.2时为 A_1 亚类;其值大于1.2时,归属为 A_2 亚类。本期碱长花岗岩Y/Nb比值为1.25~2.2,同样在Nb-Y-Ce图解(图8a)上,大多数样品落入 A_2 区。在 $Al_2O_3-SiO_2$ 、 R_1-R_2 及 $(Y + Nb)-Rb$ 构造判别图解(图8b~d)上,样品大部分落入造山期后花岗岩区域中,表明岩石为地壳伸展背景下的产物。

兴蒙造山带古生代构造格局主要受控于古亚洲洋的演化。大兴安岭地区在古生代期间经历了额尔古纳、兴安、松嫩等微地块之间的碰撞拼合演化过程。额尔古纳地块与兴安地块沿塔源—喜桂图断裂于早古生代碰撞拼合为一体(葛文春等,2005),两者的联合体沿北东向于贺根山—嫩江一带与松嫩地块拼贴。近年有资料表明嫩江地区莫尔根河组火山岩(353 Ma)(李宝民,2012)及大兴安岭北段扎兰屯地区的高钾—钾玄质钙碱性、准铝质—弱过铝质I型—分异I型花岗岩类(365~350 Ma)(钱程等,2018)为岛弧岩浆活动形成的,结合形成于洋壳俯冲构造背景下红山梁地区的含钠闪石糜棱岩(352 Ma)及蘑菇气地区的辉长岩(353 Ma)(刘宾强,2016),反映碰撞拼合应发生在~350 Ma之后。

研究区南部的霍龙门地区和全胜林场地区发现的与碰撞相关的二长花岗岩(351.5 Ma)(李成禄等,2013)、二长—正长花岗岩(322.2 Ma)(崔芳华等,2013)和碰撞—拼合的直接产物蓝片岩(334 Ma)(张兴洲,1992),以及嫩江—黑河构造带新开岭群变质地层中发现的与兴安—松嫩地块碰撞拼贴有关的

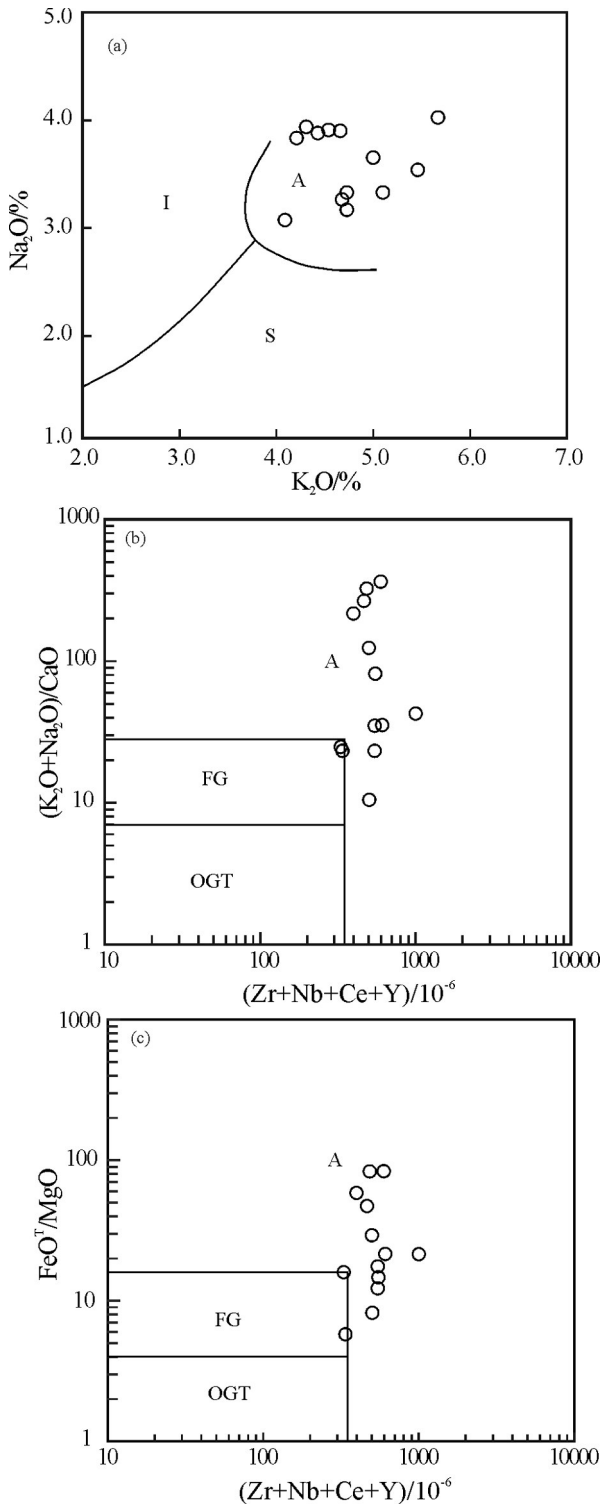


图7 多宝山碱长花岗岩类型判别图解(a, 据 Collins et al.,1982; b, c, 据 Whalen et al.,1987)

FG—分异的长英质花岗岩; NG—未分异的M, I和S型花岗岩

Fig.7 Discrimination diagram for granite types in Duobaoshan (a, after Collins et al.,1982; b, c, after Whalen et al.,1987)

FG—Fractional granitoids; NG— Nonfractionated M—I—S—type granitoids

花岗质糜棱岩(324.5 Ma)(汪岩等,2013),还有以贺根山—嫩江—黑河一线为界,由早石炭世的北海南陆转变为晚石炭世的北陆南海(刘永江等,2011)的海陆变迁事件,均说明两地块的拼贴时间应为早石炭世早期—晚石炭世早期。在此之后,形成时间为260~315 Ma,广泛出露于兴安地块嫩江—黑河一带的大黑山、小山屯、固河与松木山岩体(孙德等有,2000),达音河岩体(赵院冬等,2013),巴升河岩体(陈会军等,2019),新晟、新立与泥鳅河岩体(杨红章等,2019)等造山运动之后的I型和A型花岗岩体,标志着两地块碰撞拼合(造山运动)的结束。研究区碱长花岗岩形成于300~310 Ma,且具有造山后花岗岩的特点,应为该花岗岩带的一部分。

部分学者根据小兴安岭西北部新开岭—科洛杂岩216 Ma的变质年龄(苗来成等,2003)及贺根山蛇绿岩的辉长岩时代290~298 Ma(Miao et al., 2008),认为两地块的碰撞拼合应发生在早中生代,晚古生代的岩浆活动与碰撞前洋壳俯冲板片的局部走滑拉分作用有关,但难以解释近些年新发现造山后花岗岩的大面积出露。这些花岗岩体可能不单是俯冲板片的断离造成的,其形成应与兴安地块和松嫩地块拼合后地壳的伸展减薄有关。研究表明,在古亚洲洋闭合后,区域上仍存在贺根山弧后盆地俯冲消减运动。同样小规模造山运动可以在后造山阶段存在(Zhang et al.,2011),并且该区域在石炭纪—二叠纪存在从俯冲到碰撞的构造旋回(Jian et al.,2010),贺根山地区与俯冲作用有关的辉长岩(290~298 Ma)可能为此次构造旋回的产物。

综上所述,本文认为兴安地块与松嫩地块在早石炭世早期—晚石炭世早期处于碰撞—拼合阶段,而后转入造山后伸展阶段。

6 结 论

(1) 定年结果显示2件碱长花岗岩样品的加权年龄为(300.3±2.0)Ma(MSWD=0.22, n=20)和(307.2±1.8)Ma(MSWD = 0.74, n=24),结合前人研究成果,表明其形成于晚石炭世,属兴安造山带海西运动晚期岩浆活动的产物。

(2) 综合矿物学及地球化学特征,多宝山碱长花岗岩具A型花岗岩特征,并可细分为A₂型。

(3) 多宝山碱长花岗岩形成于造山后的伸展构造

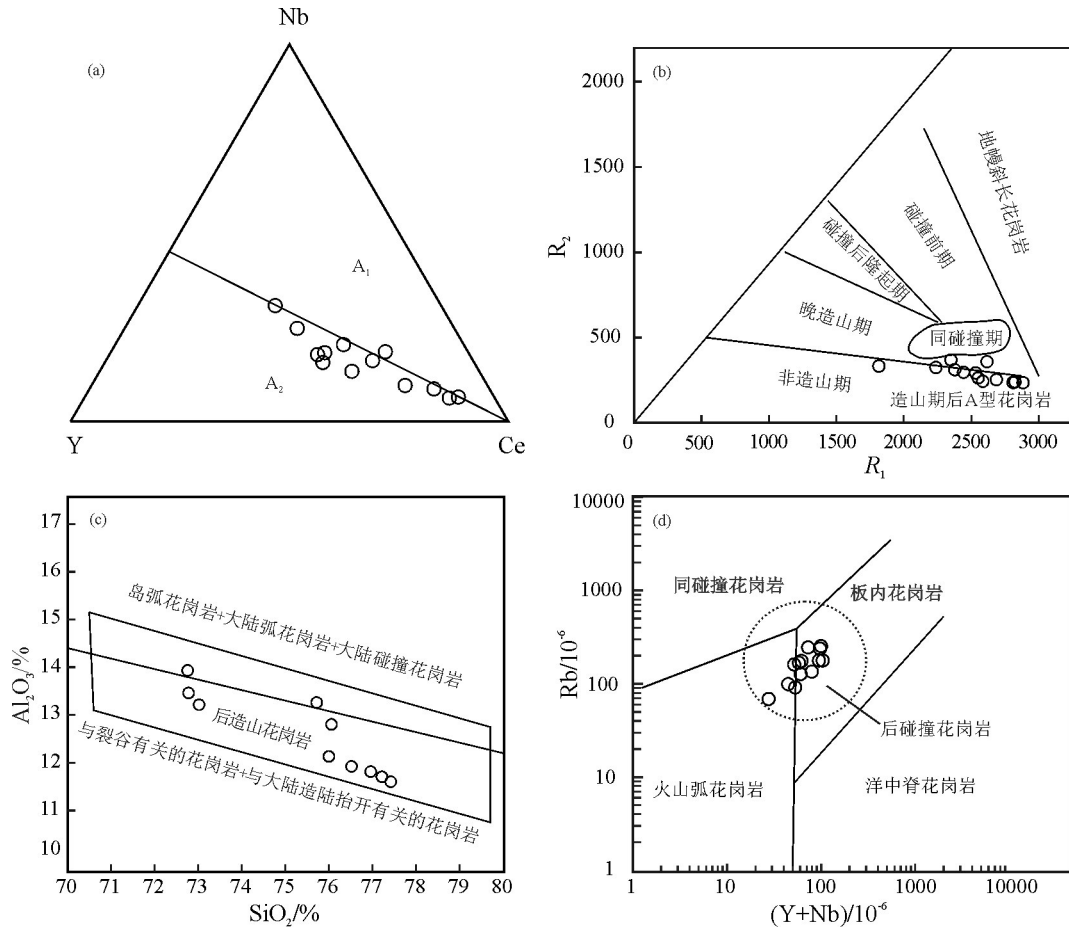


图8 多宝山碱长花岗岩构造环境判别图

(a, 据 Eby, 1992; b, 据 Maniar et al., 1989; c, 据 Whalen, 1987; d, 据 Pearce, 1984)

Fig. 8 Tectonic discrimination diagrams for the alkali-feldspar granite in Duobaoshan

(a, after Eby, 1992; b, after Maniar et al., 1989; c, after Whalen, 1987; d, after Pearce, 1984)

环境,并标志着兴安与松嫩地块碰撞拼合的结束。

References

- Anderson J L, Bender E E. 1989. Nature and origin of Proterozoic A-type granitic magmatism in the southwestern United States of America[J]. *Lithos*, 23(1/2):19-52.
- Breiter K. 2011. Nearly contemporaneous evolution of the A- and S-type fractionated granites in the Krušné hory/Erazgebirge Mts., Central Europe[J]. *Lithos*, 151:105-121.
- Chen B, Jahn B M, Wildes S, Xu B. 2000. Two contrasting Paleozoic magmatic belts in northern Inner Mongolia, China: Petrogenesis and tectonic implications[J]. *Tectonophysics*, 328(1/2): 157-182.
- Chen Huijun, Cui Tianri, Qian Cheng, Li Linchuan, Chen Jingsheng, Li Wei, Wu Xinwei, Jiang Bin, Si Qiuliang, Qin Tao, Tang Zhen, Zhang Yujin, Guo Wei. 2019. Zircon U-Pb geochronology of Bashenghe pluton in northern Daxinganling mountains: Geological implications[J]. *Geology and Resources*, 28(5): 405-412 (in Chinese with English abstract)
- Chen Peirong, Zhang Bangtong, Kong Xinggong, Cai Bicong, Ling Hongfei, Ni Qisheng. 1998. Geochemical characteristics and tectonic implication of Zhaibe A-type granitic intrusives in South Jiangxi Province[J]. *Acta Petrologica Sinica*, 14(3): 289-298(in Chinese with English abstract).
- Clemens J D, Holloway J R, White A J R. 1986. Origin of an A-type granite: Experimental constraints[J]. *American Mineralogist*, 71(3-4):317-324.
- Collins W J, Beams S D, White A J R, Chappell B W. 1982. Nature and origin of A-type granites with particular reference to southeastern Australia[J]. *Contrib. Mineral. Petrol.*, 80(2): 189-200.
- Cui Fanghua, Zheng Changqing, Xu Xuechun, Yao Wengui, Shi Lu, Xu Juan, Xu Jiulei. 2013. Late Carboniferous magmatic activities in the Quanshenglinchang area, Great Xing'an Range: Constrains on the timing of amalgamation between Xing'an and Songnen Massifs[J]. *Acta Geologica Sinica*, 87(9): 1247-1263(in Chinese with English abstract).

- Eby G N. 1992. Chemical subdivision of the A-type granitoids: Petrogenetic and tectonic implications[J]. *Geology*, 20(7): 644.
- Ge Wenchun, Wu Fuyuan, Zhou Changyong, Abdel Rahman A A. 2005. The age of Tahe granite in the north of the Daxinganling Mountains and its constraints on the structural allocation of the Erguna Block[J]. *Chinese Science Bulletin*, 50(12): 1239–1247(in Chinese).
- Gu Lianxing. 1990. Geological features, petrogenesis and metallogeny of A-type granites[J]. *Geological Science and Technology Information*, 9(1): 25–31(in Chinese).
- Hong Dawei, Wang Shiguang, Han Baofu, Jin Manyuan. 1995. Classification of structural environments of alkaline granites and their identification marks[J]. *Science in China(Series B)*, 25(4): 418–426(in Chinese).
- Jackson S E, Pearson N J, Griffin W L, Belousovai E A. 2004. The application of laser ablation-inductively coupled plasma-mass spectrometry to in situ U-Pb zircon geochronology[J]. *Chemical Geology*, 211(1/2): 47–69.
- Jia Xiaohui, Wang Qiang, Tang Gongjian. 2009. A-type granites: Research progress and implications[J]. *Geotectonica et Metallogenia*, 33(3): 465–480(in Chinese with English abstract).
- Jian Ping, Liu Dunyi, Alfred Kröner, Brian F Windley, Shi Yuruo, Zhang Wei, Zhang Fuqin, Miao Laicheng, Zhang Liqiao, Dondov Tomurhuu. 2010. Evolution of a Permian intraoceanic arc-trench system in the Solonker suture zone, Central Asian Orogenic Belt, China and Mongolia[J]. *Lithos*, 118(1/2): 169–190.
- Kang Lei, Xiao Peixi, Gao Xiaofeng, Xi Rengang, Yang Zaichao. 2016. Chronology, geochemistry and petrogenesis of monzonitic granite and quartz diorite in Mangai area: Its inspiration to early Paleozoic tectonic-magmatic evolution of the southern Altyn Tagh[J]. *Acta Petrologica Sinica*, 32(6): 1731–1748(in Chinese with English abstract).
- King P L, White A J R, Chappell B W, Allen C M. 1997. Characterization and origin of aluminous A-type granites from the Lachlan Fold Belt, Southeastern Australia[J]. *Journal of Petrology*, 38(3):371–391.
- Li Baomin. 2012. Geochemistry and Tectonic Background of the Volcanic Rocks of Early Carboniferous Moergenhe Formation in Nenjiang Area, Heilongjiang Province[D]. Changchun: Jilin University(in Chinese with English abstract).
- Li Chenglu, Qu Hui, Zhao Zhonghai, Xu Guozhan, Wang Zhuo, Zhang Jianfeng. 2013. Zircon U-Pb ages, geochemical characteristics and tectonic implications of Early Carboniferous granites in Huolongmen area, Heilongjiang Province[J]. *Geology in China*, 40(3): 859–868(in Chinese with English abstract).
- Li Huaikun, Geng Jianzhen, Hao Shuang, Zhang Yongqing, Li Huimin. 2009. Determination of U-Pb isotope ages in zircon by laser ablative multi-receiver plasma mass spectrometer (LA-MC-ICPMS) [J]. *Acta Mineralogica Sinica*, 29(S1):600–601(in Chinese).
- Li Shaunglin, Ouyang Ziyuan. 1998. Tectonic framework and evolution of Xing'anling-mongolian orogenic belt (Xmob) and its adjacent region[J]. *Marine Geology & Quaternary Geology*, 18(3): 46–55 (in Chinese with English abstract).
- Li Tong. 1994. Element abundances of China's continental crust and its sedimentary layer and upper continental crust[J]. *Geochimica*, 23(2): 140–145(in Chinese with English abstract).
- Li Xiaowei, Mo Xuanxue, Zhao Zhidan, Zhu Dicheng. 2010. A discussion on how to discriminate A-type granite[J]. *Geological Bulletin of China*, 29(2/3): 278–285(in Chinese with English abstract).
- Liu Binjiang. 2016. Study on the Paleozoic Evolution of the Nenjiang-Heihe Tectonic Belt, Northern Great Xing'an Range[D]. Changchun: Jilin University(in Chinese with English abstract).
- Liu Changshi, Chen Xiaoming, Chen Peirong, Wang Rucheng, Hu Huan. 2003. Subdivision, discrimination criteria and genesis for A-type rock suites[J]. *Geological Journal of China Universities*, 9(4): 573–591(in Chinese with English abstract).
- Liu Yongjiang, Zhang Xingzhou, Chi Xiaoguo, Wen Quanbo, Liang Chenyue, Han Guoqing, Zhao Limin, Zhao Yingli. 2011. Deformation and tectonic layer division of the Upper Paleozoic in Daxing'anling Area[J]. *Journal of Jilin University(Earth Science Edition)*, 41(5): 1304–1313(in Chinese with English abstract).
- Liu Yongjiang, Zhang Xingzhou, Jin Wei, Chi Xiaoguo, Wang Chengwen, Ma Zhihong, Han Guoqing, Wen Quanbo, Zhao Yingli, Wang Wendi, Zhao Xifeng. 2010. Late paleozoic tectonic evolution in northeast China[J]. *Geology in China*, 37(4): 943–951 (in Chinese with English abstract).
- Loiselle M C, Wones D R. 1979. Characteristics and origin of anorogenic granites[J]. *Geological Society of America, Abstracts with Programs*, 11(7): 468
- Ludwig K R. 1991. Isoplot-A plotting and regression program for radiogenic-isotope data [J]. *US Geological Survey Open-File Report*, 39: 91–445.
- Ma Yongfei, Liu Yongjiang, Peskov A Yu, Wang Yan, Song Weimin, Zhang Yujin, Qian Cheng, Liu Tongjun. 2021. Paleozoic tectonic evolution of the eastern Central Asian Orogenic Belt in NE China[J]. *China Geology*.doi: 10.31035/cg2021079. 204.
- Maniar P D, Piccoli P M. 1989. Tectonic discrimination of granitoids[J]. *Geological Society of America Bulletin*, 101(5): 635–643.
- McDonough W F, Sun S S. 1995. The Composition of the Earth[J]. *Chemical Geology*, 120(3/4): 223–253.
- Miao Laicheng, Fan Weiming, Zhang Fuqin, Liu Dunyi, Jian Ping, Shi Guanghai, Tao Hua, Shi Yuruo. 2003. SHRIMP zircon geochronology and its implications on the Xinkailing-Keluo complex, northwestern of Lesser Xing'an Range[J]. *Chinese Science Bulletin*, 48(22): 2315–2323(in Chinese).

- Miao Laicheng, Fan Weiming, LiuDunyi, ZhangFuqin, ShiYuruo, Guo Feng. 2008. Geochronology and geochemistry of the Hegenshan ophiolitic complex: Implications for late-stage tectonic evolution of the Inner Mongolia–Daxinganling Orogenic Belt, China[J]. *Journal of Asian Earth Sciences*, 32(5/6): 348–370.
- Pearce J A, Harris N B W, Tindle A G. 1984. Trace element discrimination diagrams for the tectonic interpretation of granitic rocks[J]. *Journal of Petrology*, 25(4):956–983.
- Peccerillo R, Taylor S R. 1976. Geochemistry of eocene calc–alkaline volcanic rocks from the Kastamonu area, Northern Turkey[J]. *Contributions to Mineralogica & Petrology*, 58(1): 63–81.
- Qian Cheng, Lu Lu, Qin Tao, Li Linchuan, Chen Huijun, Cui Tianri, Jiang Bin, Na Fuchao, Sun Wei, Wang Yan, Wu Xinwei, Ma Yongfei. 2018. The early Late–Paleozoic granitic magmatism in the Zalantun region, northern Great Xing'an Range, NE China: Constraints on the timing of amalgamation of Erguna–Xing'an and Songnen Blocks[J]. *Acta Geologica Sinica*, 92(11): 2190–2214(in Chinese with English abstract).
- Qu Hui, Li Chenglu, Zhao Zhonghai, Wang Zhuo, Zhang Jianfeng. 2011. Zircon U–Pb ages and geochemical characteristics of the granites in Duobaoshan area, Northeast Da Hinggan Mountains[J]. *Geology in China*, 38(2): 292–300(in Chinese with English abstract).
- Rapp R P, Watson E B. 1995. Dehydration melting of metabasalt at 8–32 kbar: Implications for continental growth and crust–mantle recycling [J]. *Journal of Petrology*, 36(4): 891–931.
- Sui Zhenmin, Chen Yuejun. 2011. Zirconsaturation temperatures of granites in eastern Great Xing'an Range, and its geological signification[J]. *Global Geology*, 30(2): 162–172(in Chinese with English abstract).
- Sui Zhenmin, Ge Wenchun, Xu Xuechun, Zhang Jiheng. 2009. Characteristics and geological implications of the Late Paleozoic post–orogenic Shierzhan granite in the Great Xing' an Range[J]. *Acta Petrologica Sinica*, 25(10): 2679–2686(in Chinese with English abstract).
- Sun Deyou, Wu Fuyuan, Li Huimin, Lin Qiang. 2000. Emplacement age of the post–orogenic A–type granites in northwestern Lesser Xing' an Range, and its relationship to the east–ward extension of Suolunshan–Hegenshan–Zhalaite collisional suture zone [J]. *Chinese Science Bulletin*, 46(5): 427–432(in Chinese).
- Sun S S, Modonough W F. 1989. Chemical and isotopic systematics of oceanic basalts: Implications for mantle composition and processes[J]. *Geological Society London Special Publications*, 42(1): 313–345.
- Watson E B. 1979. Zircon saturation in felsic liquids: Experimental results and applications to trace element geochemistry[J]. *Contributions to Mineralogy and Petrology*, 70(4): 407–419.
- Wang Yang, Yang Xiaoping, Na Fuchao, Zhang Guangyu, Kang Zhuang, Liu Yingcai, Zhang Wenlong, Mao Zhaoxia. 2013. Determination and geological implication of the granitic mylonite in nenjiang–heihe tectonic belt[J]. *Geology and Resources*, 22(6): 452–459(in Chinese with English abstract).
- Whalen J B, Carri K L, Chappell B W. 1987. A–type granites: Geochemical characteristics, discrimination and petrogenesis[J]. *Contributions to Mineralogy and Petrology*, 95(4): 407–419.
- Wu Suoping, Wang Meiyang, Qi Kaijing. 2007. Present situation of researches on A–type granites a review[J]. *Acta Petrologica et Mineralogica*, 26(1): 57–66(in Chinese with English abstract).
- Wu Yuanbao, Zheng Yongfei. 2004. Genesis of zircon and its constraints on interpretation of U–Pb age[J]. *Chinese Science Bulletin*, 49(16): 1589–1604(in Chinese).
- Wu Fuyuan, Sun Deyou, Li Huimin, Jahn B, Wilde S. 2002. A–type granites in northeastern China: Age and geochemical constraints on their petrogenesis[J]. *Chemical Geology*, 187(1/2), 143–173.
- Xu Wenxi, Li Chenglu. 2018. Middle Jurassic granites in Huolongmen area, northeastern Daxing' anling mountains: Zircon U–Pb age, geochemistry and tectonic implications[J]. *Geology and Resources*, 27(6):522–530 (in Chinese with English abstract).
- Yang Hongzhang, Chen Jiafu, Liu Junlai, Liu Bo, Gao Menghao, Chen Miaoqi, Su Li. 2019. Zircon U–Pb ages and geochemical characteristics of Late Carboniferous plutons in the southeastern Xing' an block and their tectonic implications[J]. *Acta Geologica Sinica*, 93(9): 2226–2244(in Chinese with English abstract).
- Yin Zhigang, Gong Zhaomin, Zhang Yuelong, Han Yu, Wang Yang, Cao Zhongqiang, Li Haina, Li Min. 2018. Geochronology, geochemistry and geological significance of the Early Cretaceous alkali feldspar granites in the Yilehuli Mountain, Da Hinggan, Mountain[J]. *Geological Bulletin of China*, 37(6):1061–1074 (in Chinese with English abstract).
- Zhan Huanli, Liu Xuguang, Liu Haiyang, Zhu Chunyan. 2011. Petrological evidence of Paleozoic marine basin closure in Duobaoshan of Heilongjiang[J]. *Global Geology*, 30(1): 18–27(in Chinese with English abstract).
- Zhang Lei, Lü Xinbiao, Liu Ge, Chen Jun, Chen Chao, Gao Qi, Liu Hong. 2013. Characteristics and genesis of continental back–arc A–type granites in the eastern segment of the inner Mongolia–Da Hinggan Mountains orogenic belt[J]. *Geology in China*, 40(3): 869–884(in Chinese with English abstract).
- Zhang Qi, Ran Hao, Li Chengdong. 2012. A–type granite: What is the essence? [J]. *Acta Petrologica Sinica*, 31(4): 621–626(in Chinese with English abstract).
- Zhang X H, Mao Q, Zhang H F, Zhai M G, Yang Y H, Hu Z C. 2011. Mafic and felsic magma interaction during the construction of high–K calc–alkaline plutons within a metacratonic passivemargin: The Early Permian Guyang batholith from the northern North China Craton[J]. *Lithos*, 125(1/2):569–591.
- Zhang Xingzhou, Zhou Jianbo, Chi Xiaoguo, Wang Chenwen, Hu Daqian. 2008. Late Paleozoic tectonic–sedimentation and

- petroleum resources in northeastern China[J]. Journal of Jilin University(Earth Science Edition), 38(5): 719-725(in Chinese with English abstract).
- Zhang Xingzhou. 1992. Evidence from the Caledon Suture Zone of the Heilongjiang Rock Series- Gujiamusi Block[J]. Journal of Changchun Institute of Geology, 22(s): 94- 101(in Chinese with English abstract).
- Zhang Yanlong, Ge Wenchun, Gao Yan, Chen Jingsheng, Zhao Lei. 2010. Zircon U- Pb ages and Hf isotopes of granites in Longzhen area and their geological implications[J]. Acta Petrologica Sinica, 26(4):1059-1073(in Chinese with English abstract).
- Zhao Yuandong, Zhao Jun, Wang Kuiliang, Che Jiying, Wu Datian, Xu Fengming, Li Shichao. 2013. Characteristics of the Late Carboniferous post- orogenic Dayinhe intrusion in the northwest of the Xiao Hinggan Mountains and their geological implications[J]. Acta Petrol. Mineral, 32(1): 63- 72(in Chinese with English abstract).
- Zhao Zhenhua, Xiong Xiaolin, Wang Qiang, Qiao Yulou. 2008. Some aspects on geochemistry of Nb and Ta[J]. Geochimica, 37(4): 304- 320(in Chinese with English abstract).
- Zhao Zhi, Chi Xiaoguo, Pan Shiyu, Liu Jianfeng, Sun Wei, Hu Zhaochu. 2010. Zircon U- Pb LA- ICP- MS dating of Carboniferous volcanics and its geological significance in the northwestern Lesser Xing' an Range[J]. Acta Petrologica Sinica, 26(8):2452-2464 (in Chinese with English abstract).
- Zhao Liangliang, Xu Fuzhong, Zhang Yan, Ni Bin, Ma Xiaohui. 2021. Zircon U- Pb chronology of the Heilongjiang complex in Mudanjiang area: Geological implication[J]. Geology and Resources, 30(4): 405-413(in Chinese with English abstract).
- Zhou Changyong, Wu Fuyuan, Ge Wenchun, Sun Deyou, Abdel Rahman A A, Zhang Jiheng, Cheng Ruiyu. 2005. Age, geochemistry and petrogenesis of the cumulate gabbro in Tahe, northern Da Hinggan Mountain[J]. Acta Petrologica Sinica[J], 21(3): 763-775(in Chinese with English abstract).
- 陈会军, 崔天日, 钱程, 李林川, 陈井胜, 李伟, 吴新伟, 江斌, 司秋亮, 秦涛, 唐振, 张渝金, 郭威. 2019. 大兴安岭北段巴升河岩体锆石 U-Pb 年代学及其地质意义[J]. 地质与资源, 28(5):405-412.
- 陈培荣, 章邦桐, 孔兴功, 蔡笔聪, 凌洪飞, 倪琦生. 1998. 赣南寨背 A 型花岗岩体的地球化学特征及其构造地质意义[J]. 岩石学报, 14(3): 289-298.
- 崔芳华, 郑常青, 徐学纯, 姚文贵, 施璐, 李娟, 徐久磊. 2013. 大兴安岭全胜林场地区晚石炭世岩浆活动研究:对兴安地块与松嫩地块拼合时间的限定[J]. 地质学报, 87(9):1247-1263.
- 葛文春, 吴福元, 周长勇, Abdel Rahman A A. 2005. 大兴安岭北部塔河花岗岩体的时代及对额尔古纳地块构造归属的制约[J]. 科学通报, 12(50):1239-1247.
- 顾连兴. 1990. A 型花岗岩的特征、成因及成矿[J]. 地质科技情报, 9(1): 25-31.
- 洪大卫, 王式洗, 韩宝福, 靳满元. 1995. 碱性花岗岩的构造环境分类及其鉴别标志[J]. 中国科学(B辑), 25(4): 418-426.
- 贾小辉, 王强, 唐功建. 2009. A 型花岗岩的研究进展及意义[J]. 大地构造与成矿学, 33(3): 465-480.
- 康磊, 校培喜, 高晓峰, 奚仁刚, 杨再朝. 2016. 茫崖二长花岗岩、石英闪长岩的年代学、地球化学及岩石成因:对阿尔金南缘早古生代构造-岩浆演化的启示[J]. 岩石学报, 32(6): 1731-1748.
- 黎彤. 1994. 中国陆壳及其沉积层和上陆壳的化学元素丰度[J]. 地球化学, 23(2): 140-145.
- 李宝民. 2012. 黑龙江省嫩江地区莫尔根河组火山岩的岩石学、地球化学特征及其构造背景[D]. 长春: 吉林大学.
- 李成禄, 曲晖, 赵忠海, 徐国战, 王卓, 张俭峰. 2013. 黑龙江霍龙门地区早石炭世花岗岩的锆石 U-Pb 年龄、地球化学特征及构造意义[J]. 中国地质, 40(3):859-868.
- 李怀坤, 耿建珍, 郝爽, 张永清, 李惠民. 2009. 用激光烧蚀多接收器等离子体质谱仪(LA-MC-ICPMS)测定锆石 U-Pb 同位素年龄的研究[J]. 矿物学报, 29(S1):600-601.
- 李双林, 欧阳自远. 1998. 兴蒙造山带及邻区的构造格局与构造演化[J]. 海洋地质与第四纪地质, 18(3):46-55.
- 李小红, 莫宣学, 赵志丹, 朱弟成. 2010. 关于 A 型花岗岩判别过程中若干问题的讨论[J]. 地质通报, 29(2/3): 278-285.
- 刘宾强. 2016. 大兴安岭北段嫩江-黑河构造带古生代演化研究[D]. 长春: 吉林大学.
- 刘昌实, 陈小明, 陈培荣, 王汝成, 胡欢. 2003. A 型岩套的分类、判别标志和成因[J]. 高校地质学报, 9(4): 573-591.
- 刘永江, 张兴洲, 金巍, 迟效国, 王成文, 马志红, 韩国卿, 温泉波, 赵英利, 王文弟, 赵喜峰. 2010. 东北地区晚古生代区域构造演化[J]. 中国地质, 37(4):943-951.
- 刘永江, 张兴洲, 迟效国, 温泉波, 梁琛岳, 韩国卿, 赵立敏, 赵英利. 2011. 大兴安岭地区上古生界变形特征及构造层划分[J]. 吉林大学学报(地球科学版), 41(5): 1304-1313.
- 苗来成, 范蔚茗, 张福勤, 刘敦一, 简平, 施光海, 陶华, 石玉若. 2003. 小兴安岭西北部新开岭-科洛杂岩锆石 SHRIMP 年代学研究及其意义[J]. 科学通报, 48(22): 2315-2323.
- 钱程, 陆露, 秦涛, 李林川, 陈会军, 崔天日, 江斌, 那福超, 孙巍, 汪岩, 吴新伟, 马永非. 2018. 大兴安岭北段扎兰屯地区晚古生代早期花岗岩浆作用——对额尔古纳-兴安地块和松嫩地块拼合时限的制约[J]. 地质学报, 92(11): 2190-2214.
- 曲晖, 李成禄, 赵忠海, 王卓, 张俭峰. 2011. 大兴安岭东北部多宝山区花岗岩锆石 U-Pb 年龄及岩石地球化学特征[J]. 中国地质, 38(2):292-300.
- 隋振民, 陈跃军. 2011. 大兴安岭东部花岗岩类锆石饱和温度及其地质意义[J]. 世界地质, 30(2): 162-172.
- 隋振民, 葛文春, 徐学纯, 张吉衡. 2009. 大兴安岭十二站晚古生代后造山花岗岩的特征及其地质意义[J]. 岩石学报, 25(10):2679-2686.
- 孙德有, 吴福元, 李惠民, 林强. 2000. 小兴安岭西北部造山后 A 型花岗岩的时代及与索伦山-贺根山-扎赉特碰撞拼合带东延的关

附中文参考文献

- 系[J]. 科学通报, 45(20): 2217-2222.
- 汪岩, 杨晓平, 那福超, 张广宇, 康庄, 刘英才, 张文龙, 毛朝霞. 2013. 嫩江-黑河构造带中花岗质糜棱岩的确定及地质意义[J]. 地质与资源, 22(6): 452-459.
- 吴锁平, 王海英, 戚开静. 2007. A型花岗岩研究现状及其述评[J]. 岩石矿物学杂志, 26(1): 57-66.
- 吴元保, 郑永飞. 2004. 锆石成因矿物学研究及其对U-Pb年龄解释的制约[J]. 科学通报, 49(16): 1589-1604.
- 徐文喜, 李成禄. 2018. 大兴安岭东北部霍龙门地区中侏罗世花岗岩——锆石U-Pb年龄、地球化学特征及构造意义[J]. 地质与资源, 27(6):522-530.
- 杨红章, 陈家富, 刘俊来, 刘博, 邵梦豪, 陈妙琦, 苏犁. 2019. 兴安地块东南缘晚石炭世侵入岩的锆石U-Pb年代学、地球化学特征及构造意义[J]. 地质学报, 93(9): 2226-224.
- 尹志刚, 官兆民, 张跃龙, 韩宇, 王阳, 曹忠强, 李海娜, 李敏. 2018. 大兴安岭伊勒呼里山早白垩世碱长花岗岩年龄、地球化学特征及其地质意义[J]. 地质通报, 37(6):1061-1074.
- 张磊, 吕新彪, 刘阁, 陈俊, 陈超, 高奇, 刘洪. 2013. 兴蒙造山带东段大陆弧后A型花岗岩特征与成因[J]. 中国地质, 40(3): 869-884.
- 张旗, 冉焱, 李承东. 2012. A型花岗岩的实质是什么?[J]. 岩石矿物学杂志, 31(4): 621-626.
- 张兴洲, 周建波, 迟效国, 王成文, 胡大千. 2008. 东北地区晚古生代构造-沉积特征与油气资源[J]. 吉林大学学报(地球科学版), 38(5): 719-725.
- 张兴洲. 1992. 黑龙江岩系——古佳木斯地块加里东缝合带的证据[J]. 长春地质学院学报, 22(s): 94-101.
- 张彦龙, 葛文春, 高妍, 陈井胜, 赵磊. 2010. 龙镇地区花岗岩锆石U-Pb年龄和Hf同位素及地质意义[J]. 岩石学报, 26(4):1059-1073.
- 赵焕利, 刘旭光, 刘海洋, 朱春艳. 2011. 黑龙江多宝山古生代海盆闭合的岩石学证据[J]. 世界地质, 30(1): 18-27.
- 赵亮亮, 徐福忠, 张岩, 倪斌, 马晓辉. 2021. 牡丹江地区黑龙江杂岩锆石U-Pb年代学特征及地质意义[J]. 地质与资源, 30(4):405-413.
- 赵院冬, 赵君, 王奎良, 车继英, 吴大天, 许逢明, 李世超. 2013. 小兴安岭西北部晚石炭世造山后达音河岩体的特征及其地质意义[J]. 岩石矿物学杂志, 32(1): 63-72.
- 赵振华, 熊小林, 王强, 乔玉楼. 2008. 铋与钼的某些地球化学问题[J]. 地球化学, 37(4): 304-320.
- 赵芝, 迟效国, 潘世语, 刘建峰, 孙巍, 胡兆初. 2010. 小兴安岭西北部石炭纪地层火山岩的锆石LA-ICP-MSU-Pb年代学及其地质意义[J]. 岩石学报, 26(8):2452-2464.
- 周长勇, 吴福元, 葛文春, 孙德有, Abdel Rahman A A, 张吉衡, 程瑞玉. 2005. 大兴安岭北部塔河堆晶辉长岩体的形成时代、地球化学特征及其成因[J]. 岩石学报, 21(3): 763-775.